

CAN SOOT PRIMARY PARTICLE SIZE BE DETERMINED USING LASER-INDUCED INCANDESCENCE?

Thomas M. Ticich, A. Brock Stephens, Department of Chemistry,
Centenary College of Louisiana, Shreveport, Louisiana, 71134

Randy L. VanderWal, Nyma@NASA-Lewis Research Center,
Cleveland, Ohio 44315

laser-induced incandescence, soot, primary particle size

ABSTRACT

We have obtained temporally-resolved laser-induced incandescence (LII) signals from different size primary particles produced by diffusion flames of methane, ethane, ethylene, and acetylene. These results represent the first direct comparison between primary particle sizes based on optical measurements and those directly measured through TEM. Two measures of the temporal decay of the LII signal reveal a correlation with primary particle size. Comparison between primary particle sizes based on the calibrations using the temporal analysis of the LII signal and TEM measurements reveal agreement within the growth region and very late in the oxidation region within an ethylene gas-jet diffusion flame. Significant differences exist at intermediate positions which likely represent the effects of cluster-cluster aggregation within the oxidation region.

INTRODUCTION

Soot surface growth rather than nucleation has been found to dominate soot mass yield (1-4). Essential in characterizing the rate of soot growth and assessing theoretical models is the soot surface area. For example, soot mass proceeds via hydrogen abstraction creating a surface radical site in preparation for acetylene addition to the site (5). In such a process, the mass addition rate will depend upon total surface area in addition to the number of potential reactive sites (6).

Several parameters characterizing soot mass growth can be readily measured optically, such as soot volume fraction (f_v), velocity and temperature. Optical measurements are advantageous because they are non-intrusive and take place in real time. Optical, in-situ determination of primary particle size would further facilitate measuring soot mass growth and oxidation rates per unit surface area. The current methodology for primary particle size determination is through analysis of transmission electron microscopy (TEM) micrographs of thermophoretically sampled soot, an intrusive and time-intensive process (1-4).

Largely due to its high temporal and spatial resolution, laser-induced incandescence (LII) has advanced f_v measurements to a wide range of combustion processes. Theoretical models of LII predict that the temporal evolution of the signal after the excitation laser pulse is dependent upon primary particle size (7-11). This is physically sensible given that the temporal evolution of the LII signal is dependent upon the cooling of the primary particles predominantly through conduction and convection, processes dependent upon surface area. Thus the work presented here seeks to explore the potential of LII for determining primary particle size. Given the number of assumptions utilized in present LII theoretical models regarding the physical and structural properties of the laser-heated soot (7-11), we adopted an empirical approach to seek a correlation between the temporal decay rate of the LII signal and primary particle size as determined from analysis of transmission electron micrographs of thermophoretically sampled soot.

EXPERIMENTAL

A variety of laminar gas-jet diffusion flames produced by different fuels and flowrates were used to produce a wide range of primary particle sizes at similar temperatures and near the maximum in their growth history. Table 1 lists the different fuels, flow conditions, sampling heights above the burner, primary particle sizes and local temperatures for each of the four flames studied. The flame temperatures reported were measured by thermocouples employing rapid

insertion (72) with subsequent radiation correction (73). Each gas-jet diffusion flame was supported on a 10.5 mm I.D. nozzle surrounded by an air coflow through a 101 mm diameter honeycomb. A chimney with windows for optical access served to stabilize the flame and provide shielding from room drafts.

For LII measurements, the 1064 nm light from a pulsed Nd:YAG laser was formed into a 500 μm -wide sheet and directed through the flame. LII signals were relayed through a quartz optical fiber to a monochromator fitted with a photomultiplier tube (PMT) as the detector. The signal collection system has a spectral bandwidth of 12 nm and a transverse spatial resolution of 1 mm. Time-resolved PMT signals were sampled using a 500 MHz digital oscilloscope which also covered 200 individual temporal scans.

Thermophoretic sampling provided soot samples for transmission electron microscopy. Probe residence times within the flames ranged from 30-60 ms depending on the soot volume fraction. TEM grids with ultrathin substrates aided visualization of the sampled soot. TEM micrographs were analyzed for primary particle size using commercial image processing software.

RESULTS AND DISCUSSION

Calibration Development

Figure 1 shows the time-resolved LII signal for three flames at the longest detection wavelength studied, 600 nm. Qualitatively similar data were obtained at shorter detection wavelengths but the largest observed variation in the temporal evolution of the LII signal occurred at 600 nm. Two analysis methods based on a theoretical model of the LII signal have been reported recently for extracting primary particle size from LII data (10,11). The first method uses the ratio of signal intensity (integrated over a specified time duration after the excitation laser pulse) at two detection wavelengths (10). An advantage of this method, according to the theoretical model, is reduced sensitivity to differences in ambient flame temperature. Analysis of our data in this manner, however, gave a nonmonotonic relationship between the ratio and primary particle size, which would result in a given signal ratio indicating two different particle sizes.

The second method of analysis is based on the ratio of signal intensity at a single detection wavelength with the signal integrated over selected electronic gate durations (11). Figure 2 shows the results of this method of analysis applied to the time-resolved LII signals from the different primary particle sizes. Because the method uses a limited portion of the experimental data, we also sought to utilize all the experimental data by fitting the signal decay to a mathematical function. Our analysis showed significant disagreement between the decaying portion of the time-resolved data and a single exponential fit. Far better agreement was observed using a double exponential fit. The double exponential curve fits were applied between data points where the signal intensity was 10% and 90% of the peak value. The cooling process of the laser-heated soot reflects the concurrent contributions of radiation, conduction, and convection that vary with time after the excitation laser pulse (7-12). Thus, the dual time constants may reflect different timescales associated with the different cooling mechanisms. Using the fast decay rate did not give a monotonic relation with increasing primary particle size. Figure 2 plots the second decay rate value (obtained by fitting the time-resolved LII signals for the various diffusion flames) against their primary particle size. The dynamic range and monotonic relationship exhibited by the analysis methods whose results are plotted in Figure 2 give each potential as an empirical calibration curve for inferring primary particle size based on the temporal decay rate of the LII signal in other systems.

Application

Motivated by the need for measuring primary particle size to determine soot mass growth and oxidation rates per unit surface area (1-6), we tested the utility of the calibration curve for determining primary particle size. Time-resolved LII data were obtained at different heights above the burner along the axial streamline within the

ethylene flame and subsequently fit to a double exponential and also analyzed using the method of gate ratios. Using the calibration curves presented in Figure 2, the measured long-time decay rates were translated into primary particle sizes.

The trend exhibited in both calibration plots is similar to the predicted results published in reference 10. Although the acetylene point is consistent with this trend, it was not used because of the different flame temperature which will affect the cooling processes (see Table 1). Given the uncertainty in the functional form of a curve-fit, line segments connecting the calibration points were used for interpolation. The ethane-ethylene segment was extrapolated to obtain primary particle sizes from points beyond the ethylene calibration point.

Figure 3 presents the results. In order to test the accuracy of the predictions, thermophoretic sampling measurements were performed followed by TEM microscopy and subsequent primary particle size analysis. These results are also plotted in Figure 3. While good agreement is observed at heights above the burner (HAB) of 40, 45, 80, and 85 mm, pronounced differences exist between 55 and 75 mm HAB, where the values measured from the TEM micrographs are significantly below the predicted values. Note that the agreement observed at 50 mm reflects its being used as a calibration point.

The deviations observed in the oxidation regions likely result from the aerosol process of cluster-cluster aggregation (14). Soon after the formation of aggregates within the growth region, clustering of aggregates can begin. This process will continue to occur throughout the growth and well into the oxidation regions of the flame. TEM images in the annular region of the flame show that as the aggregates cluster, they not only become larger but also more dense and compact (15,16). This is consistent with our own observations along the axial streamline. TEM images of soot aggregates collected at 40, 60, and 80 mm HAB show that the open branched chain appearance of aggregates within the growth region do qualitatively change to a more densely-packed, less open structure in the oxidation region. Such a structure could decrease the rate of cooling of individual primary particles (or fused units) through self-absorption of emitted thermal radiation and inhibition of conductive and convective cooling. Hence the optical measurement, which reflects the rate of temperature decrease of the laser-heated soot, would also be affected. Upon sufficient oxidation, the aggregates eventually crumble, so that the primary particles within the fragments return to a more open structure similar to that at their initial coalescence early within the growth region. At this stage, good agreement between the optical and TEM measurements would be expected, as observed. It could be argued that the oxidation process itself could slow the rate of cooling of the laser-heated soot. Localized burning of the soot could contribute to locally elevated temperatures of the particles. Given the agreement between temperatures within sooting flames measured via optical pyrometry and thermocouples, however, this appears to be a minor contribution.

Another soot particle property that could affect the cooling process is the degree of primary particle connectivity. The degree of connectivity is a maximum at the peak of the soot growth region. Increasing primary particle connectivity would increase the effective primary particle size thus decreasing the cooling rate. Since our calibration points are at the peak of the growth region where the connectivity effects are maximum, this would underpredict primary particle sizes at other heights. The observed agreement between the predicted and experimental results within the soot growth region and the fact that the predicted results lie above the TEM measured values indicate that primary particle connectivity does not significantly impact the results presented here. The overprediction of the primary particle size relative to the TEM values within the oxidation region is also consistent with this postulate.

CONCLUSIONS

Our results suggest that LII can be used to predict primary particle size under certain conditions. Local flame temperatures will affect the cooling rate of the particle and thus the optical signal. Therefore, the flame temperature in the calibration system and the system to which it is applied must be similar in this empirical approach. Cluster-cluster aggregation will also affect the cooling rate

and the predicted primary particle sizes if it differs between the two systems. Particle-particle connectivity does not appear to be a significant factor in the results presented here.

These results represent the first direct comparison between primary particle sizes based on optical measurements and those directly measured through TEM. Predictions based on the temporal decay rate of the LII signal produce better agreement than those based on the gate ratio method.

ACKNOWLEDGEMENTS

This work was supported through NASA contract NAS3-27186 with Nyma Inc. Dr. Ticich and Mr. Stephens gratefully acknowledge support through the Ohio Aerospace Institute ASEE summer faculty fellowship and accompanying student program.

REFERENCES

1. Harris, S.J.; Weiner, A.M. *Combust. Sci. and Technol.* **1984**, *38*, 75.
2. Megardis, C.M. *Combust. Sci. and Technol.* **1989**, *66*, 1.
3. Sunderland, P.B.; Faeth, G.M. *Combust. and Flame* **1996**, *105*, 132.
4. Sunderland, P.B.; Koylu, U.O.; Faeth, G.M. *Combust. and Flame* **1995**, *100*, 310.
5. Frenklach, M.; Wang, H. 23rd Symposium (International) on Combustion, The Combustion Institute, Pittsburgh, PA. 1990; 1559.
6. Howard, J.B.; 23rd Symposium (International) on Combustion, The Combustion Institute, Pittsburgh, PA. 1990; 1107.
7. Melton, L.A. *Appl. Opt.* **1984**, *23*, 2201.
8. Hofeldt, D.L. Society of Automotive Engineers, Warrendale, PA, 1993; SAE Tech. Paper 930079.
9. Dasch, C.J. *Appl. Opt.* **1984**, *23*, 2209.
10. Mewes, B.; and Seitzman, J.M. *Appl. Opt.* **1997**, *36*, 709.
11. Will, S.; Schraml, S.; and Leipertz, A. 23rd Symposium (International) on Combustion, The Combustion Institute, Pittsburgh, PA. 1996; 2277.
12. Eisner, D.A.; Rosner, D.E. *Combust. and Flame*, **1985**, *61*, 153.
13. Smyth, K.C.; Miller, J.H.; Dorfman, R.C.; Mallard, W.G.; Santoro, R.J. *Combust. and Flame*, **1985**, *62*, 157.
14. Puri, R.; Richardson, T.F.; Santoro, R.J.; *Combust. and Flame*, **1993**, *92*, 320.
15. Dobbins, R.A.; Megaridis, C.M. *Langmuir* **1987**, *3*, 254.
16. Koylu, U.O.; Faeth, G.M.; Farias, T.L.; Carvalho, M.G. *Combust. and Flame*, **1995**, *100*, 621.

Fuel	Flow Rate (sccm)	Axial Height (mm)	Primary Size TEM (nm)	Temperature (K)
Methane	350	50	13.4 +/- 1.6	1750
Ethane	255	61	24.4 +/- 2.1	1700
Ethylene	231	50	33.3 +/- 3.5	1600
Acetylene	200	50	59.7 +/- 3.9	1200

Table 1. Summary of experimental conditions and primary particle sizes.

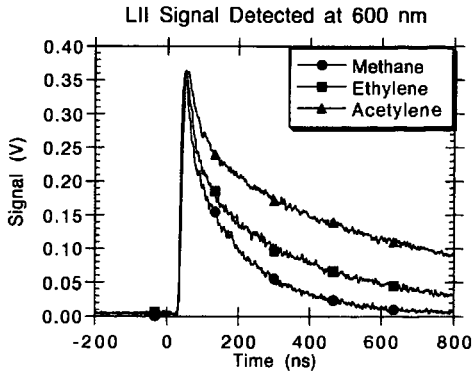


Figure 1. Time-resolved LII signals produced by the different size primary particles in the various flames.

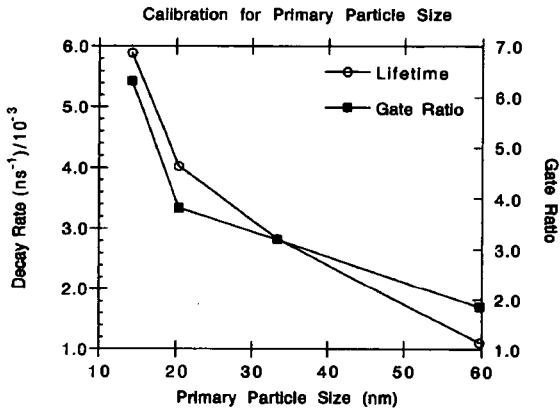


Figure 2. Correlation between measured primary particle size and the second decay rate and gate ratio describing the temporally resolved LII signal.

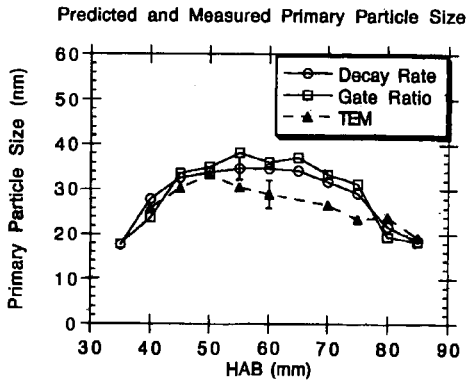


Figure 3. Comparison between the predicted primary particle size based on the optical measurements and interpreted using the calibration curves in Figure 2 and direct measurements from TEM micrographs.